

Thermal behavior of a small salinity-gradient solar pond with wall shading effect

M.R. Jaefarzadeh *

Faculty of Engineering, Civil Engineering Department, Ferdowsi University of Mashhad, P.O. Box 91775-1111, Mashhad, Iran

Received 5 September 2003; received in revised form 6 May 2004; accepted 27 May 2004

Available online 1 July 2004

Communicated by: Associate Editor Aliakbar Akbarzardeh

Abstract

The thermal behavior of a small-scale salinity-gradient solar pond has been studied in this paper. The model of heat conduction equation for the non-convective zone has been solved numerically with the boundary conditions of the upper and lower convective zones. The variation of the solar radiation, during a year, and its attenuation in the depth of the pond has been discussed. The wall shading area for a vertical wall square pond has been elaborated and its effect on the reduction of the sunny area has been included in the model. The temperature variation of the storage zone has been calculated theoretically and compared with the experimental results. The sensitivity analysis demonstrates the importance of the side and bottom insulation and the thickness of the non-convective zone, as well as the wall shading effect on the performance of the pond. The application of several loading patterns gives an overall efficiency of 10% for the small pond.

© 2004 Elsevier Ltd. All rights reserved.

Keywords: Salinity-gradient solar pond; Solar energy

1. Introduction

A salinity-gradient solar pond consists of three distinct zones: the upper convective zone (UCZ) which is uniform with a density close to the seawater, the middle or non-convective zone (NCZ) which has a relatively linear density gradient, and the lower convective zone (LCZ) which is uniform with a density close to the saturated brine.

The solar radiation encountering the surface of a solar pond is transferred to the lower zone and heats it up. The middle layer acts as a thermal insulator, preventing the loss of energy, collected at the LCZ, except by conduction, which is a slow process. The en-

ergy, stored at the LCZ, may be utilized by a heat exchanger.

The utility of a solar pond depends on the amount of its thermal energy storage, and on the construction costs plus maintenance expenses. Therefore, an accurate analysis of its thermal behavior will be vital. The thermal performance of a solar pond is a function of solar irradiation, heat losses from the sides to the surroundings and from the LCZ towards the upper layers, ultimate storage capacity, and the effectiveness of the heat exchanger system. All the characteristics of different zones of a solar pond may vary during the time; and for a perfect analysis, the mass and energy balance equations should be solved simultaneously. However, the process of the variations of the parameters is so much slow that for a rather correct estimation each equation may be solved separately.

The thermal energy balance for a large solar pond was first investigated by Weinberger (1964). He had neglected the thicknesses of the upper and lower

* Fax: +98-511-8436-433.

E-mail address: jafarjad@ferdowsi.um.ac.ir (M.R. Jaefarzadeh).

Nomenclature

A, A_e, A_{sh} , total, sunny and shaded areas of the pond (m ²)	Q_R total radiation energy entering into the LCZ (W)
A_s peripheral area of the LCZ (m ²)	Q_{up}, Q_s, Q_G energy losses from the LCZ to the NCZ, the sides and the ground (W)
b side of the square pond (m)	Q_L extracted energy from the pond (W)
c salt concentration (kg/m ³)	R reflection coefficient
C_p specific heat of the fluid (J/kg °C)	T temperature (°C)
D_U, D_N, D_L thicknesses of the UCZ, NCZ and LCZ (m)	t time
$E(Z, t)$ solar radiation absorbed in the body of the pond (W/m ² /m)	X, Z horizontal and vertical coordinates
h local time	δ, ϕ angles of declination and latitude
h_s hour of sunrise	γ surface azimuth angle
I, I_R solar radiation and direct radiation (W/m ²)	θ_i, θ_r angles of incidence (zenith angle) and refraction of beam radiation
k, k_G, k_s fluid, ground and side coefficients of heat conduction (W/m °C)	θ_v angle of incidence of beam radiation with normal to a vertical plane
L_D the length of the day (h)	ρ fluid density (kg/m ³)
n the day of the year, index of refraction	ω hour angle
	τ transmissivity function

convective zones and solved the energy equation analytically, by a superposition method. Rabl and Nielsen (1975) developed the one-zone model of Weinberger into a two-zone pond. In their model, the thickness of the UCZ had been overlooked.

Analytical methods are useful for simple studies, however, when the boundary conditions are complex, or the variations of thermophysical parameters are to be considered, numerical models should be utilized. There have been several attempts for the numerical solution of energy equation in the literature. For example, Hull (1980), Hawlader and Brinkworth (1981), and Rubin et al. (1984) have applied a finite difference method, while Jayadev and Henderson (1979), and Panahi et al. (1983) have used a finite element technique.

In the small vertical wall solar ponds, the shading of walls has a decisive role on reducing the sunny area of the pond, and its thermal behavior. Lund and Routti (1984) studied the feasibility of the solar pond heating for the northern cold climates. In their model, the effect of the shading of walls for a circular pond had been considered, theoretically. However, in the present study, the wall shading effect has been regarded for the thermal analysis of a small-scale rectangular solar pond, in the city of Mashhad (36°16'N, 59°37'E) and thereby, the pond performance has been studied theoretically, and verified experimentally for one year.

2. Mathematical formulation

In a vertical system of coordinates with Z measured as positive downward and $Z = 0$ at the surface of the

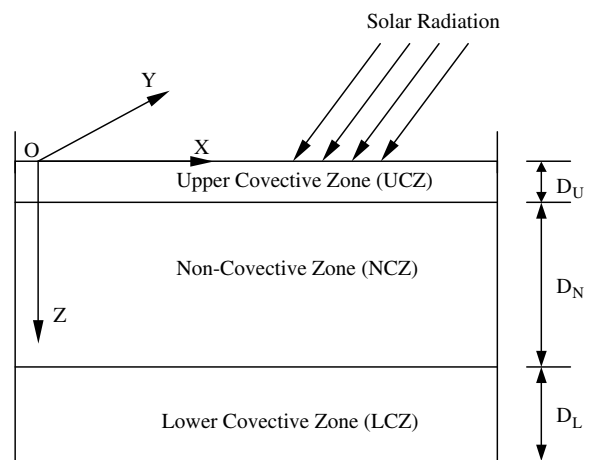


Fig. 1. Schematic view of a solar pond.

pond, Fig. 1, the transient equation of heat conduction in one dimension for the non-convective zone will be written as (Sukhatme, 1984; Tabor and Weinberger, 1981)

$$\rho C_p \frac{\partial T}{\partial t} = \frac{\partial}{\partial Z} \left(k \frac{\partial T}{\partial Z} \right) + E(Z, t) \quad D_U \leq Z \leq D_U + D_N \quad (1)$$

where ρ is the fluid density in kg/m³, C_p the specific heat of the fluid in J/kg °C, T the temperature in Celsius degrees, t the time, k the coefficient of heat conduction in W/m °C, E the solar radiation absorbed in the body of

the pond, D_U the thickness of the surface layer, and D_N the thickness of the gradient layer.

The thermophysical properties of a saline solution pond, in terms of temperature T , and salt concentration c in kg/m^3 , are given by (Kaufmann, 1960)

$$k = 0.5553 - 0.0000813c + 0.0008(T - 20) \quad (2)$$

$$\rho = 998 + 0.65c - 0.4(T - 20) \quad (3)$$

$$C_p = 4180 + 4.396c + 0.0048c^2 \quad (4)$$

The absorbed radiation energy is obtained from

$$E(Z, t) = \frac{-d}{dZ} \left[\frac{A_e + A_{sh}\xi}{A} I_R(Z, t) \right] \quad (5)$$

where A is the total area of the pond in m^2 , A_e the sunny or effective radiation area A_{sh} the shaded area ξ is a fraction of direct or beam radiation, that is changed to diffusive radiation at the shaded area, due to the reflection of the walls and the bottom, and $I_R(Z, t)$ is the direct radiation flux in W/m^2 that reaches a depth of Z at any time t .

According to Rubin et al. (1984), the diffusive radiation is about 15% of the total energy of the solar radiation at noon and 40% of the total energy at sunrise or sunset. Samimi (1986) assumed the diffusive radiation as 10% of the direct radiation at sunny hours and 30% at cloudy hours of the day. In this study, we have assumed $\xi = 30\%$, having taken into account the effect of diffusive radiation on the shaded area.

There are two boundary conditions at the upper interface, $Z = D_U$ and the lower interface, $Z = D_U + D_N$.

For the upper boundary, the temperature of the UCZ has been assumed as constant and equal to the ambient temperature.

$$T = T_{amb} \quad (6)$$

This assumption has been applied in most similar models and confirmed by experimental observations.

For the lower boundary condition, the temperature T_L of the LCZ has been assumed constant, to be calculated from the energy conservation equation. In Fig. 2, for a control volume of the LCZ, with a thickness of D_L , it may be written

$$\rho C_p A D_L \frac{\partial T_L}{\partial t} = Q_R - Q_{up} - Q_s - Q_G - Q_L \quad (7)$$

In Eq. (7), the LHS is the time variation of thermal energy in the control volume; and in the RHS, the first term is the radiation energy entering the control volume, the second term is the energy loss to the non-convective zone at the interface, the third and fourth terms are the energy losses to the sides and ground, and the last term is the extracted energy from the solar pond, in a loading period. These terms are formulated thus

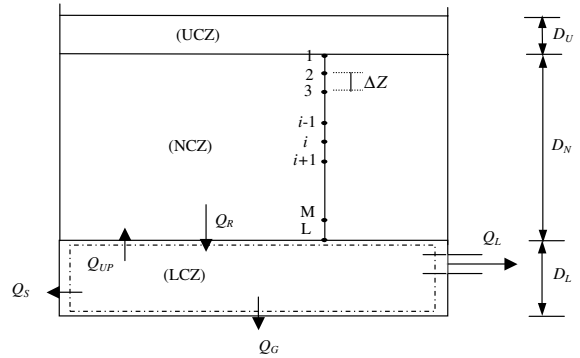


Fig. 2. Discretization of the NCZ and control volume of the LCZ.

$$Q_R = A_e I_R + A_{sh} \xi I_R = (A_e + A_{sh} \xi) I_R \quad (8)$$

$$Q_{up} = -kA \frac{\partial T}{\partial Z} \Big|_{Z=D_U+D_N} \quad (9)$$

$$Q_s = -k_s A_s \frac{\partial T}{\partial X} \Big|_{side} \quad (10)$$

and

$$Q_G = -k_G A \frac{\partial T}{\partial Z} \Big|_{Z=D_U+D_N+D_L} \quad (11)$$

where A_s is the side area of the control volume, D_L the thickness of the LCZ, k_s and k_G the coefficients of heat conduction from the sides and bottom of the pond.

The initial condition has been obtained by assuming a uniform temperature profile at the start of the pond operation.

3. Numerical solution

Eq. (1), is classified as a parabolic, second order, partial differential equation. One of the best methods for the solution of this kind of equations is the so-called Crank–Nicolson scheme. In Fig. 2, the NCZ has been divided into M parts, and for a node located at $Z_i = (i - 1)\Delta Z + D_U$, $i = 2, 3, \dots, M$, at time $t = n\Delta t$, $n = 1, 2, \dots$, Eq. (1) can be discretized thus

$$\begin{aligned} \rho_i C_{pi} \frac{T_i^{n+1} - T_i^n}{\Delta t} = & \frac{1}{2\Delta Z^2} [k_{i+1/2}(T_{i+1}^{n+1} - T_i^{n+1}) \\ & + k_{i-1/2}(T_{i-1}^{n+1} - T_i^{n+1})] \\ & + \frac{1}{2\Delta Z^2} [k_{i+1/2}(T_{i+1}^n - T_i^n) \\ & + k_{i-1/2}(T_{i-1}^n - T_i^n)] + E_i^{n+1/2} \end{aligned} \quad (12)$$

with the upper boundary as

$$T_1^n = T_{amb}^n \quad (13)$$

and the lower boundary as

$$\rho C_p A D_L \frac{(T_L^{n+1} - T_L^n)}{\Delta t} = Q_R^n - Q_{up}^n - Q_s^n - Q_G^n - Q_L^n \quad (14)$$

where

$$Q_R^n = (A_e + A_{sh}\xi)I_R^n \quad (15)$$

$$Q_{up}^n = -kA \frac{T_M^n - T_L^n}{\Delta Z} \quad (16)$$

$$Q_s^n = -k_s A_s \frac{T_W^n - T_L^n}{\Delta S} \quad (17)$$

$$Q_G^n = -k_G A \frac{T_G^n - T_L^n}{\Delta S} \quad (18)$$

In the above equations, T_L^n is the temperature of the LCZ, T_M^n the temperature of the lowest node at the gradient zone, T_G^n the temperature of the ground, T_W^n the wall temperature, and ΔS the distance at which T_W^n or T_G^n are measured.

Using Eqs. (15)–(18) in Eq. (14) and simplifying, gives the temperature of the LCZ, explicitly at the time of $n + 1$

$$T_L^{n+1} = \frac{\Delta t}{\rho C_p D_L} \left[\left(\frac{A_e + A_{sh}\xi}{A} \right) I_R^n + k \frac{T_M^n - T_L^n}{\Delta Z} + \frac{k_s A_s}{A} \frac{T_W^n - T_L^n}{\Delta S} + k_G \frac{T_G^n - T_L^n}{\Delta S} - \frac{Q_L}{A} \right] + T_L^n \quad (19)$$

The implicit system of Eq. (12) with the boundary conditions of (13) and (19) has been solved with a double sweep algorithm (Anderson et al., 1984).

4. Solar radiation

The angle of incidence of direct radiation to a horizontal plane with normal (zenith angle) is given by (Duffie and Beckman, 1980)

$$\cos \theta_i = \cos \delta \cos \phi \cos \omega + \sin \delta \sin \phi \quad (20)$$

in which δ is the angle of declination, ϕ the angle of latitude, and ω the hour angle.

The declination angle δ is defined in degrees by

$$\delta = 23.45 \sin \left(\frac{360(284 + n)}{365.25} \right) \quad (21)$$

where n is the day of the year.

The hour angle ω is an angular measure of time considered from noon based on local time h , and is defined thus

$$\omega = \frac{2\pi(h - 12)}{24} \quad (22)$$

The angle of the incidence of direct radiation to a vertical plane with the normal is given through

$$\cos \theta_v = -\sin \delta \cos \phi \cos \gamma + \cos \delta \sin \phi \cos \gamma \cos \omega + \cos \delta \sin \gamma \sin \omega \quad (23)$$

The surface azimuth angle γ is the angle made in the horizontal plane between the line due south and the projection of the normal to the surface on the horizontal plane. By convention, it will be positive if the normal is west of south, and negative if east of south.

The hour of sunrise is given via

$$h_s = 6 + \frac{12}{\pi} \text{Arc sin}(-\tan \phi \tan \delta) \quad (24)$$

The day length in hours is obtained from

$$L_D = \frac{24}{\pi} \text{Arc cos}(-\tan \phi \tan \delta) \quad (25)$$

5. Attenuation of solar radiation in a solar pond

Some part of the solar radiation, I , reaching the pond surface, is reflected back. The remainder I_s , is obtained from

$$I_s = (1 - R)I \quad (26)$$

where R , is the coefficient of reflection and can be calculated from (Wang and Akbarzadeh, 1983)

$$R = \frac{1}{2} \left[\frac{\sin^2(\theta_i - \theta_r)}{\sin^2(\theta_i + \theta_r)} + \frac{\tan^2(\theta_i - \theta_r)}{\tan^2(\theta_i + \theta_r)} \right] \quad (27)$$

where θ_i is the angle of incidence (zenith angle), θ_r the angle of refraction and

$$\sin \theta_i = n \sin \theta_r \quad (28)$$

in which n is the index of refraction ($n = 1.33$ for water).

The solar radiation, penetrating into the water body, is decayed exponentially with depth, as fluid layers absorb energy. The rate of decay or transmissivity is a function of the wavelength of the radiation and for the whole spectrum of wavelengths can be expressed as (Rabl and Nielsen, 1975)

$$\tau = \sum_{j=1}^4 \eta_j \exp \left(\frac{-\mu_j Z}{\cos \theta_r} \right) \quad (29)$$

in which

Wavelength	η	μ
0.2–0.6	0.237	0.032
0.6–0.75	0.193	0.45
0.75–0.9	0.167	3
0.9–1.2	0.179	35

The reduction of solar irradiation caused by salt concentration, radiation propagation in water-layers, bottom and wall reflection, and water turbidity has been

investigated by many researchers in a series of publications. A complete review can be found in references (Wang and Seyed-Yagoobi, 1994; Srinivasan and Guha, 1987). However, the validity and reliability of the recommended equations have not been examined in practice, yet. Moreover, a lot of parameters ought to be measured accurately, for the application of those equations.

Akbarzadeh and Ahmadi (1980) summarized the above mentioned effects in a coefficient of $\theta_o = 0.83$. Green et al. (1987) measured $\theta_o = 0.8$, for a solar pond in Portugal. In order to analyze the performance of a 240 m² pond in Banglore, Srinivasan (1990) used a similar value for θ_o . In the present study, we have assumed a coefficient of $\theta' = 0.85$. This coefficient when multiplied by $(1 - R)$ becomes very close to the value of θ_o that was suggested by Akbarzadeh and Ahmadi. The final form of the radiation equation is

$$I_R = (1 - R)\theta'I \tag{30}$$

and its derivative to depth is

$$\begin{aligned} \frac{dI_R}{dZ} &= (1 - R)\theta'I \frac{\partial \tau}{\partial Z} \\ &= (1 - R)\theta'I \sum_{j=1}^4 \frac{-\eta_j \mu_j}{\cos \theta_r} \exp\left(-\mu_j \frac{Z}{\cos \theta_r}\right) \end{aligned} \tag{31}$$

In Fig. 3, the variation of $\psi = (1 - R)\theta'$, τ and $(\tau\psi)$ has been plotted for a period of one year. The value of τ has been plotted for $Z = 0.7$ m which is the position of the lower interface in our experimental solar pond. It is seen that ψ varies between 0.8 and 0.88, however, the value of $\tau = 0.37$ is, approximately, constant. Consequently, $(\tau\psi)$ is in the range of 0.3–0.34. Kishore and Kumar (1996), in a 6000 m² solar pond, measured $\tau\psi = 0.434$. They

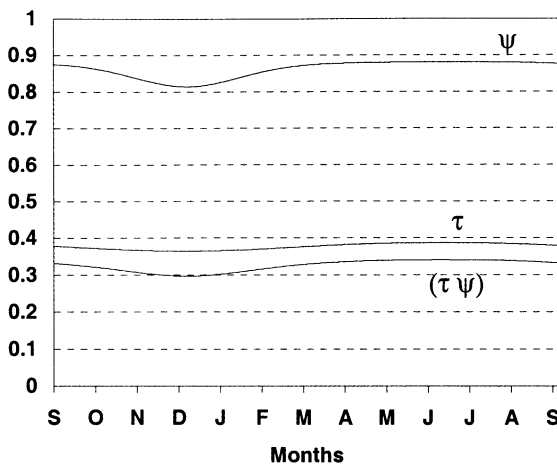


Fig. 3. Variation of the effective coefficients in reduction of irradiation during a year.

defined $\tau\psi = 0.2$ for a relatively opaque pond to $\tau\psi = 0.45$ for a transparent pond.

6. Effective area of a solar pond

One of the parameters in the reduction of sunny area in a vertical wall solar pond is its wall shading effect. This is very important for the small ponds in lab-scale size. In the present work, we study this effect in a square pond.

In Fig. 4, AB_1 is the shadow of the normal AB with a length of l . The ray BB_1 makes an incident angle θ_i , with the normal to the plane of XAY and an angle of θ_v with the normal to the plane of YAZ . If the normal AB is placed in a fluid with an index of refraction n , the point B_1 will move to B_2 , and the angles θ_i and θ_v change to θ_r and θ'_v , respectively. The shade length of AB is $l' = AB_2$ with an angle of α obtained from

$$\sin \alpha = \frac{A_1 B_1}{AB_1} = \frac{BB_1 \cos \theta_v}{BB_1 \sin \theta_i} = \frac{\cos \theta_v}{\sin \theta_i} \tag{32}$$

$$l' = AB_2 = AB \tan \theta_r = l \tan \theta_r \tag{33}$$

The values of θ_i , θ_v and θ_r are calculated from Eq. (20), Eq. (23) and Eq. (28).

For a square-shaped pond with a side of b and area A , as shown in Fig. 5, if the values of α and l' are known, the shaded area, A_{sh} may be obtained from

$$A_{sh} = bl' \sin \alpha + bl' \cos \alpha - l'^2 \sin \alpha \cos \alpha \tag{34}$$

and the effective area is given by

$$A_e = A - A_{sh} = b^2 - A_{sh} \tag{35}$$

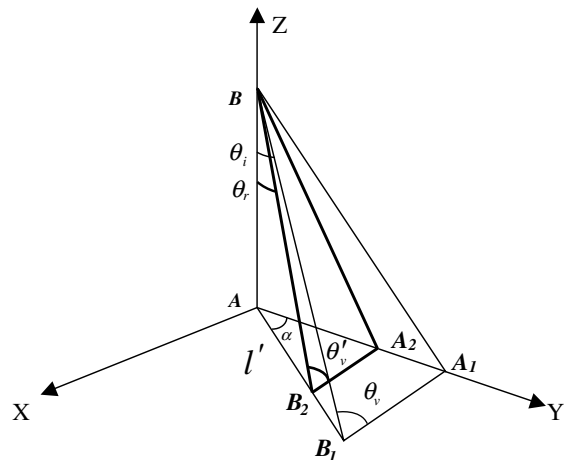


Fig. 4. The shade of normal AB in an ambient with a refraction coefficient of n .

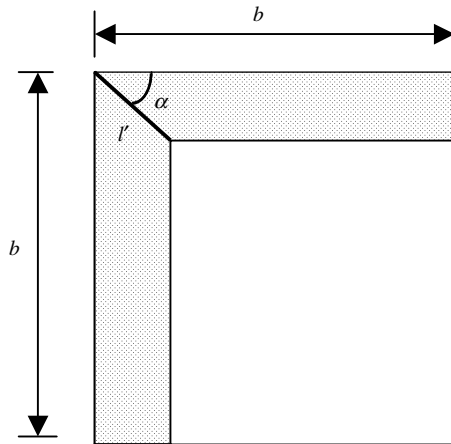


Fig. 5. Effective area and shading area in a square pond.

Therefore, the factor of the sunny area is calculated from

$$\begin{aligned} \text{SUNF} &= \frac{A_e}{A} \\ &= 1 - \left[\frac{l'}{b} \sin \alpha + \frac{l'}{b} \cos \alpha - \left(\frac{l'}{b} \right)^2 \sin \alpha \cos \alpha \right] \end{aligned} \quad (36)$$

Eqs. (34) and (35) can be substituted in Eq. (19) for the values of A_e and A_{sh} to account for the wall shading effect.

7. Description of the experimental apparatus

An experimental, lab-scale, solar pond with the area of 4 m² and a depth of 1.1 m was built in Ferdowsi University of Mashhad. The pond was double sided, with bottom and sides thermally insulated by 120 mm thick polystyrene sheets. Meteorological parameters, such as the total radiation, wind speed, relative humidity, and ambient temperature, were measured by corresponding sensors. The pond temperature was measured at 15 points spaced 7 cm in normal direction by RTD thermal sensors with an accuracy of about 0.5 °C. The monitoring system was fully automatic and the data were recorded hourly by a 32-channel data logger built at the University. Saline concentration was also measured by taking samples once a week from at least 75 stations distributed in depth spaced 1 or 2 cm in normal direction and analyzed up to three digits after decimal in gr/cm³ by a DMA35 Anton Paar density measurement instrument. The pond was filled on 11 September 1996 by the “Salinity redistribution method” and worked for four years, (Jaefarzadeh, 2000). In the present paper we report the experimental data that were measured during the first year of the pond operation.

8. Comparison between theory and experiments

In order to simulate the thermal performance of a solar pond, a computer code was developed. A time step of one day was assumed for the simulation process. The input data included geographical location, geometrical characteristics of the pond, average daily radiation, and ambient temperature, thicknesses of different layers, the thermophysical parameters of saline solution, and the initial conditions for temperature and salinity. The computer program was run for the small experimental pond, for one year, from 16 September 1996, to 15 September 1997. In this run, the thicknesses of the UCZ, NCZ, and LCZ were 0.2, 0.5 and 0.4 m, respectively. The coefficient of heat conduction for the polystyrene insulation was 0.032 W/m °C, as given by the manufacturer. The daily average temperature of the sensors, located at the insulation sheets at the bottom and sides of the pond, was used to estimate the heat losses from the perimeter of the pond. The maximum salinity was 18% at the LCZ and 1% at the UCZ.

For the calculation of the radiation angles (θ_i , θ_r and θ_v), the position of the sun during a day, and in different days of a year, had to be traced. In a direct simplification, Rabl and Nielsen (1975) assumed the sun to be at equinox at 2 p.m., and, thereby, fixed the effective angle of incidence. Here, we used a daily average irradiation, and assumed the sun at 2 p. m., for each day. Moreover, following Rabl and Nielsen, we assumed all the irradiation to be direct. The error caused by these assumptions was not more than 5%, as reported (Rabl and Nielsen, 1975).

In Fig. 6, the variation of the temperature of the LCZ, for the year 1996–1997, obtained from the computer simulation and experimental measurements has been plotted. The comparison between theory and experiment has proved quite satisfactory all year through, except during the months of June and July

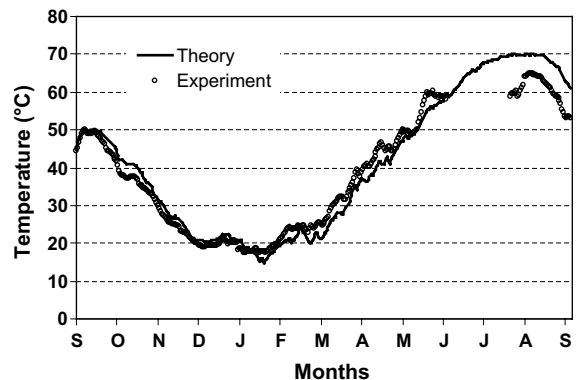


Fig. 6. Theoretical and experimental variation of the temperature of the LCZ in 1996–1997.

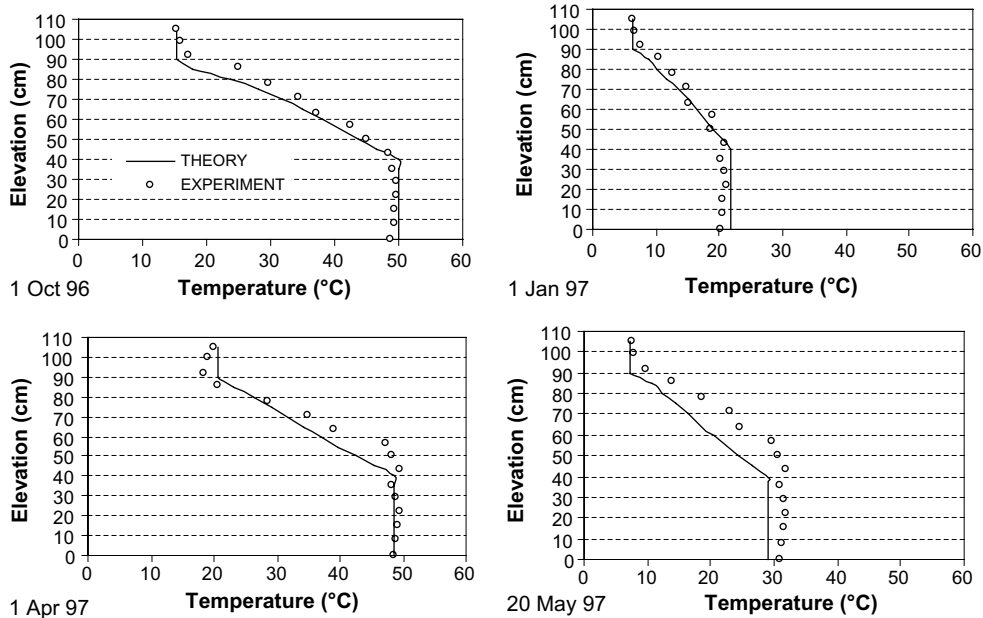


Fig. 7. Theoretical and experimental profiles of temperature distribution in depth of the solar pond at typical days of 1996–1997.

when the solar pond had been emptied and refilled because of breakage in a pipe. Therefore, this part of the experimental curve has not been completed. Based on the theoretical predictions, the solar pond could be heated up to 70 °C. However, in practice, its temperature has not increased above 65 °C. The minimum temperature of the pond, in theory, was 15 °C, while, in practice, it was 17 °C.

Fig. 7 shows the temperature profiles for a few typical days of the year. It may be concluded that the conformity in theory and experiment is generally reasonable in both the convective and non-convective zones. However, recalling that in the one dimensional heat equation model, the thickness of each zone has been fixed, there are some disagreements, at the upper and lower gradient interfaces, between the theoretical and experimental results. Precise observations of the convective motions in the LCZ and UCZ, reveals a continuous rising and falling of thermal plumes in those regions. These plumes are in part responsible for the movement of the interfaces, (Hull et al., 1989).

Fig. 8 illustrates the inward flux of irradiation to the storage zone, together with the lost fluxes, from the LCZ to the sides, ground, and upper layer. As seen, the irradiation flux varies directly with the insolation throughout the year. It decreases from September to the end of February and increases from March, to its utmost, in July. The lost energy, from the LCZ, to the upper layer is consistent with the inflow energy. It is about 80% of the total loss; the remaining 20% includes the energy losses from the sides and bottom. Therefore,

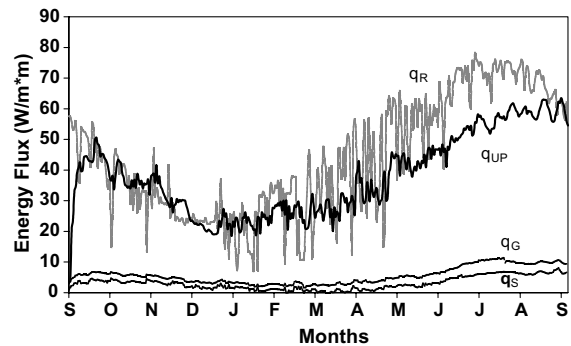


Fig. 8. Variation of the daily inward and outward energy fluxes to the LCZ.

to reduce the losses, an increase in the thickness of the NCZ is recommended.

In order to study the sensitivity of the model to different parameters, the program was run for the following cases.

- (1) In the original model, the temperature of the UCZ was identical with the ambient temperature, Eq. (13). Instead, we used the temperature of the upper sensor located in the UCZ, for the upper boundary. Fig. 9 shows the results are marginally improved; however, this is so much insignificant that the initial assumption may be applied with a satisfactory estimation.

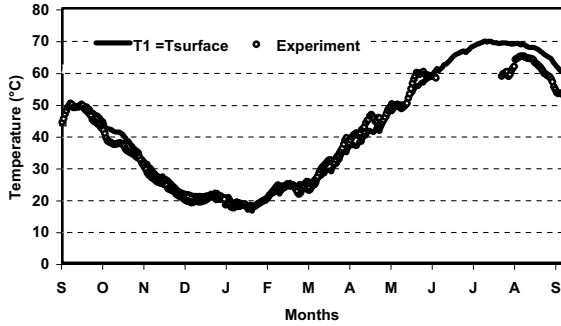


Fig. 9. Variation of the daily temperature of the LCZ for case 1.

(2) To evaluate the effect of the heat losses from the sides and bottom of the pond, first, we assumed the coefficient of the heat conduction of the insulation as zero, and then we multiplied it by a factor of 10. In Fig. 10, it is observed that the maximum and minimum temperatures, in the first case are 90 and 24 °C, and in the second case 54 and 11 °C, respectively. It may be concluded, then, that the insulation of the bottom and sides has a major con-

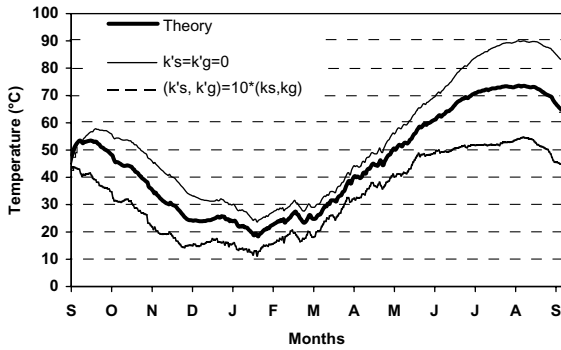


Fig. 10. Variation of the daily temperature of the LCZ for case 2.

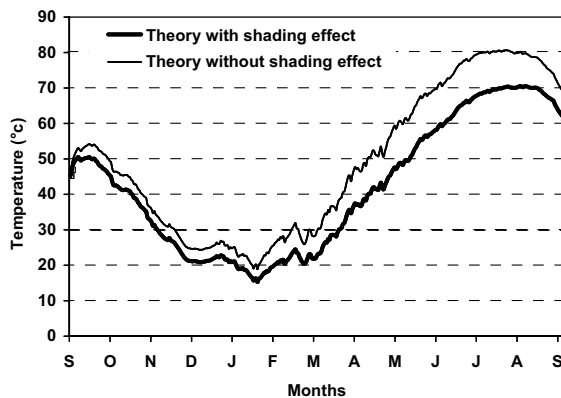


Fig. 11. Variation of the daily temperature of the LCZ for case 3.

tribution towards the thermal performance of the small pond.

(3) In the next run, we neglected the shading of the side walls by assuming $A_{sh} = 0$. This assumption enhanced the sunny area of the pond by at least 20%. Fig. 11 shows the temperature of the LCZ in comparison with the original theory including the wall shading effect. Obviously, removing the shading effect has overestimated the maximum temperature by 10 °C and the minimum by 5 °C. In other words, the reduction of the sunny area for the shading effect in small ponds will decrease the efficiency of the pond, considerably.

9. Strategy of heat removal and efficiency of the solar pond

Generally speaking, energy removal from a solar pond ought to maintain a sustainable strategy. In this regard, four different hypothetical loading patterns have been examined.

- (L1) Daily removal of energy to be 10% of daily irradiation.
- (L2) Daily removal of energy to be fixed all through the year and equal to 10% of the yearly average of daily irradiation ($\sim 18.5 \text{ W/m}^2$).
- (L3) and (L4) The same as L1 and L2, however, with 20% of energy removal.

It is to be noted that the total energy removal in case L1 are equal to case L2, and in case L3, equal to case L4. However, the distribution of energy removal in cases L1 and L3 are variable, while in cases L2 and L4 it remains constant. The variation of the temperature of the LCZ has been plotted for cases L1 and L2, in Fig. 12, and for

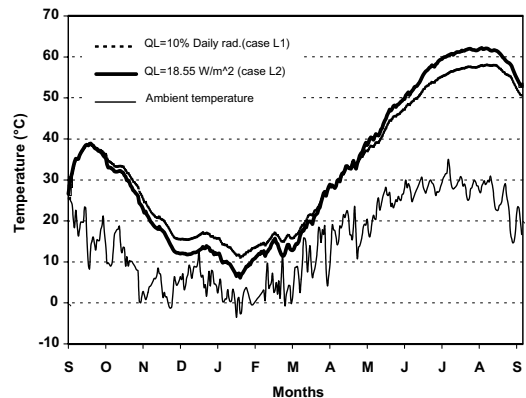


Fig. 12. Variation of the temperature of the LCZ for energy removal of 10% during a year.

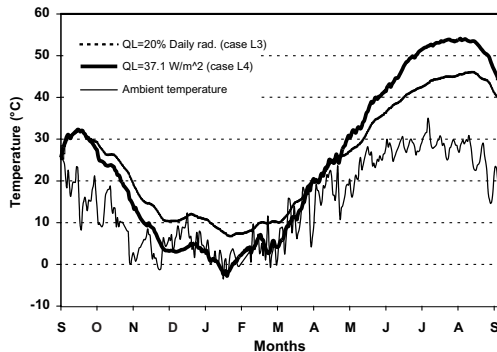


Fig. 13. Variation of the temperature of the LCZ for energy removal of 20% during a year.

cases L3 and L4, in Fig. 13, together with the ambient temperature.

As seen, in case L1, the LCZ temperature is far from the ambient temperature all through the year, whereas in case L2, during a few days of the year, the temperature of the LCZ comes close to the ambient temperature. In case L3, the LCZ temperature is very close to the ambient temperature for two months from March to the end of April. In case L4, the temperature of the LCZ drops below the ambient temperature, from December to April, for four months; and even, in late January, it falls below zero, for a few days. Consequently, only cases L1 and L2 are acceptable, and an efficiency of about 10% may be assumed for the solar pond.

Tabor (1981) has reported an efficiency of 15–25% for large solar ponds with a total depth of about 2 m. In our small solar pond, however, due to the wall shading effects, and a thin NCZ, the overall efficiency has been reduced.

10. Conclusions

The thermal behavior of a salinity-gradient solar pond has been studied in this paper. A finite difference model has been used for the discretization of the heat differential equation. The model, for the data of 1996–1997, has simulated the performance of a small-scale salinity-gradient solar pond. The results are satisfactory in both the prediction of the temperature of the LCZ and the temperature profile in the depth of the pond.

The sensitivity analysis reveals that the wall shading effect is very important in reducing the sunny area and the temperature of the LCZ. Because of the proper insulation, the heat losses from the sides and bottom of the pond are negligible. However, in order to obtain a higher temperature for the storage zone, the thickness of the NCZ should be increased.

The application of several heat removal patterns illustrates that the overall efficiency of the pond are about 10%, and a variable loading pattern is preferred.

Acknowledgements

The support of the research council of Ferdowsi University of Mashhad during the preparation of this work is kindly acknowledged. Special thanks are offered to Mrs. Sayedi for her useful comments towards the improvement of the manuscript.

References

- Akbarzadeh, A.A., Ahmadi, G., 1980. Computer simulation of the performance of a solar pond in the southern part of Iran. *Solar Energy* 24, 143–151.
- Anderson, D.A., Tannehill, J.C., Pletcher, R.H., 1984. *Computational Fluid Mechanics and Heat Transfer*. Hemisphere Publishing Corporation.
- Duffie, J.A., Beckman, W.A., 1980. *Solar Engineering of Thermal Processes*. John Wiley and sons.
- Green, A.A., Joyce, A.L.M., Collares-Pereira, M., 1987. The measurement of radiation transmission in a salt-gradient solar pond. In: *Proceedings of the Tenth Congress of the International Solar Energy Society*. Pergamon Press, Hamburg.
- Hawladar, M.N.A., Brinkworth, B.J., 1981. An analysis of the non-convective solar pond. *Solar Energy* 27, 195–204.
- Hull, J.R., 1980. Computer simulation of solar pond thermal behavior. *Solar Energy* 25, 33–40.
- Hull, J., Nielsen, C.E., Golding, P., 1989. *Salinity Gradient Solar Ponds*. CRC Press, Boca Raton, FL.
- Jaefarzadeh, M.R., 2000. On the performance of a salinity gradient solar pond. *Applied Thermal Engineering* 20, 243–252.
- Jayadev, T.S., Henderson, J., 1979. Salt concentration gradient solar ponds-modeling and optimization, *Proceedings of International Solar Energy Society*. Atlanta, pp. 1015–1019.
- Kaufmann, D.W., 1960. *Sodium Chloride*. Reinhold, New York.
- Kishore, V.V.N., Kumar, A., 1996. Solar pond: an exercise in development of indigenous technology at Kutch, India. *Energy for Sustainable Development* 3 (1), 17–28.
- Lund, P.D., Routti, J.T., 1984. Feasibility of solar pond heating for northern cold climates. *Solar Energy* 33, 209–215.
- Panahi, Z., Batty, J.C., Riley, J.P., 1983. Numerical simulation of the performance of a salt gradient solar pond, *Transaction of ASME. Journal of Solar Energy Engineering* 105, 369–374.
- Rabl, A., Nielsen, C.E., 1975. Solar ponds for space heating. *Solar Energy* 17, 1–12.
- Rubin, H., Benedict, B.A., Bachu, S., 1984. Modeling the performance of a solar pond as a source of thermal energy. *Solar Energy* 32, 771–778.
- Samimi, J., 1986. Solar energy for Iran (in: Persian). *Journal of Physics* 3, 79–105.
- Srinivasan, J., 1990. Performance of a small solar pond in the tropics. *Solar Energy* 45, 221–230.
- Srinivasan, J., Guha, A., 1987. The effect of bottom reflectivity on the performance of a solar pond. *Solar Energy* 39, 361–367.

- Sukhatme, S.P., 1984. *Solar Energy*. Tata Mc Graw-Hill Pub. Co, New Delhi.
- Tabor, H., 1981. Solar ponds. *Solar Energy* 27, 181–194.
- Tabor, H., Weinberger, Z., 1981. Non-Convecting Solar Ponds. In: Kreider, J.F., Kreith, F. (Eds.), *Solar Energy Handbook*. Mc Graw Hill, New York. Chapter 10.
- Wang, Y.F., Akbarzadeh, A.A., 1983. A parametric study on solar ponds. *Solar Energy* 30, 555–562.
- Wang, J., Seyed-Yagoobi, J., 1994. Effects of water turbidity and salt concentration levels on penetration of solar radiation under water. *Solar Energy* 52, 429–438.
- Weinberger, H., 1964. The physics of the solar pond. *Solar Energy* 8, 45–56.